

Poly(2-oxazoline) block copolymer based formulations of taxanes: effect of copolymer and drug structure, concentration, and environmental factors^{S¶}

Youngee Seo^a, Anita Schulz^{b,†}, Yingchao Han^{c,‡}, Zhijian He^a, Herdis Bludau^b, Xiaomeng Wan^a, Jing Tong^c, Tatiana K. Bronich^c, Marina Sokolsky^a, Robert Luxenhofer^{d***}, Rainer Jordan^{b**} and Alexander V. Kabanov^{a,e*}



Many current nanoformulations of taxanes are hampered by low drug-loading capacity and unfavorable physicochemical characteristics such as large particles size (>100 nm) and/or low size uniformity. We have previously reported on taxane nanoformulations, based on poly(2-oxazoline) polymeric micelles that display an extremely high taxane loading capacity (>40% w/w) and particle size below 50 nm. Previous work was based on a triblock copolymer having poly(2-butyl-2-oxazoline) as the hydrophobic block and poly(2-methyl-2-oxazoline) as the hydrophilic blocks. This paper explores the effects of various formulation parameters such as (i) the drug and polymer structure; (ii) the drug and polymer concentration; and (iii) the composition of aqueous medium on the solubilization behavior and physicochemical properties of the resulting formulations. In addition, *in vitro* anticancer activity is reported. Despite numerous variations of the hydrophobicity, polarity or addition of aromatic residues in the hydrophobic core, the triblock copolymer with the poly(2-butyl-2-oxazoline) block remains the polymer with the highest drug-loading capacity. Notably, the formulation was easily scalable with uncompromised encapsulation efficacy, loading capacity, and physicochemical properties. The taxane formulations were stable upon storage (water, saline, and dextrose solution) for 1–2 weeks and could be lyophilized and re-dispersed without compromising the formulation properties. Furthermore, the micelles remained stable upon dilution. The drug-loaded poly(2-oxazoline) micelles showed high toxicity against several cancer cell lines. Taken together, these results underscore the potential of poly(2-oxazoline) micelles as formulation excipient for taxanes and possibly other hydrophobic drugs. Copyright © 2015 John Wiley & Sons, Ltd. Supporting information may be found in the online version of this paper.

Keywords: block copolymer micelles; poly(2-oxazoline); paclitaxel; nanomedicine; drug delivery; docetaxel

* Correspondence to: Alexander V. Kabanov, Center for Nanotechnology in Drug Delivery and Division of Molecular Pharmaceutics, Eshelman School of Pharmacy, University of North Carolina at Chapel Hill, Chapel Hill, NC 27599-7362, USA. E-mail: kabanov@unc.edu

**Correspondence to: Rainer Jordan, Professur für Makromolekulare Chemie, Department Chemie, Technische Universität Dresden, Zellescher Weg 19, 01069 Dresden, Germany. E-mail: rainer.jordan@tu-dresden.de

***Correspondence to: Robert Luxenhofer, Professur für Polymere Funktionswerkstoffe, Lehrstuhl Chemische Technologie der Materialsynthese, Fakultät für Chemie und Pharmazie, Julius-Maximilians-Universität Würzburg, Röntgenring 11, 97070 Würzburg, Germany. E-mail: robert.luxenhofer@uni-wuerzburg.de

[†]Present address: Faculty of Pharmacy, Institute des Biomolécules Max Mousseron (IBMM), UMR CNRS 5247, University of Montpellier, 15 Av. C. Flahault, Montpellier, 34093 France

[‡]Present address: State Key Laboratory of Advanced Technology for Materials Synthesis and Processing, Wuhan University of Technology, Wuhan 430070 P.R. China

^S This work was supported by the Cancer Nanotechnology Platform Partnership grant (U01 CA116591) of the National Cancer Institute Alliance for Nanotechnology in Cancer. We acknowledge the assistance of the Nanomaterials Core facility of the Center for Biomedical Research Excellence (CoBRE) Nebraska Center for Nanomedicine supported by the National Institutes of Health grant (RR021937).

[¶] This article is published in *Journal of Polymers for Advanced Technologies* as a Special issue honoring Professor Stanislaw Penczek on his 80th birthday, edited by Prof. Abraham Domb and Prof. Stanislaw Slomkowski.

a Y. Seo, Z. He, X. Wan, M. Sokolsky, A. V. Kabanov
Center for Nanotechnology in Drug Delivery, Division of Molecular Pharmaceutics, Eshelman School of Pharmacy, University of North Carolina at Chapel Hill, Chapel Hill, NC, 27599-7362 USA

b A. Schulz, H. Bludau, R. Jordan
Department Chemie, Technische Universität Dresden, Zellescher Weg 19, 01069 Dresden, Germany

c Y. Han, J. Tong, T. K. Bronich
Center for Drug Delivery and Nanomedicine and Department of Pharmaceutical Sciences, College of Pharmacy, University of Nebraska Medical Center, Omaha, NE, 68198-5830 USA

d R. Luxenhofer
Functional Polymer Materials, Chair for Chemical Technology of Materials Synthesis, Department Chemistry and Pharmacy, Julius-Maximilians-Universität Würzburg, Röntgenring 11, 97070 Würzburg, Germany

e A. V. Kabanov
Laboratory of Chemical Design of Bionanomaterials, Faculty of Chemistry, M. V. Lomonosov Moscow State University, Moscow, 119992 Russia

INTRODUCTION

In modern clinical oncology, taxanes have become a first line of treatment for a variety of malignancies and are commercially the most successful chemotherapeutics in history.^[1] Taxanes cause chromosome missegregation by interfering with tubulin and microtubule function thus leading to anticancer activity in breast, ovarian, non-small cell lung, and prostate cancers.^[1–4]

The most extensively used commercial formulations for parental administration of paclitaxel (PTX) and docetaxel (DTX) such as Taxol[®] and Taxotere[®] utilize organic solvents (e.g. ethanol) and non-ionic surfactants (e.g. Tween 80[®]) to solubilize taxanes. In Taxol[®], a solvent system of 1/1 (v/v) Kolliphor EL[®] (formerly known as Cremophor EL, CrEL or polyoxyethylated castor oil) and anhydrous ethanol are utilized. In Taxotere[®], the DTX is solubilized in another polyoxyethylated surfactant, polysorbate 80 (Tween 80[®]) and ethanol.^[3] Notably, Kolliphor EL[®] and Tween 80[®] have been linked to severe side effects including but not limited to acute hypersensitivity and peripheral neuropathy. To avoid the severe adverse effects associated with Kolliphor EL[®] and Tween 80[®], a number of novel taxane formulations were developed. Some examples of these formulations are fatty acid (e.g. docosahexaenoic acid) modified PTX, vitamin E-PTX emulsion, liposomal-encapsulated PTX, poly(ethylene glycol)-poly(D,L-lactide) polymeric-micellar PTX (Genexol-PM^[5–8]), and human serum albumin-PTX complex particles (Abraxane[®]), which is widely used in the clinics.^[9] Genexol-PM is currently clinically approved in Europe and South Korea and is in advanced clinical trials in the USA. Notably, both Abraxane[®] and Genexol-PM formulations showed comparable *in vitro* cytotoxicity, higher maximum tolerated dose, improved biodistribution, higher dose without excipient-associated toxicity, and improved antitumor efficacy *in vivo* compared with commercial PTX formulation (Taxol[®]).^[8,10–12] However, clinical trials revealed more severe side effects, such as peripheral neuropathy as compared with Taxol[®]. More important, it has been shown that Abraxane[®] does not necessarily prolong progression-free survival compared with Taxol[®].^[9,13,14]

Unique characteristics of tumor microenvironment, such as drain failure of lymphatic vessels, elevated interstitial fluid pressure (IFP)^[15,16], and accumulation of collagen in the interstitial space^[17,18] limit the ability of the nanoformulations with sizes above 60 nm to penetrate through the tumor.^[19,20] It was shown that after extravasating from the leaky tumor vessel, these particles could not diffuse and remained in the perivascular region,^[21] which resulted in reduced efficacy. Specifically, Cabral *et al.* observed that only 30 nm size micelles could penetrate into poorly permeable pancreatic tumor while 50, 70, and 100 nm particles could not.^[22] Therefore, despite extensive research and a variety of reported nanoformulations, there is still a need for new formulations, which will combine high loading capacity and good overall solubility with a tunable and defined nanoparticle size below 50 nm.

Amphiphilic block copolymers have been widely studied as carriers for taxanes. The ability of amphiphilic block copolymers to solubilize hydrophobic compounds is attributed to their nanoscopic core/shell structure. The water-insoluble block in amphiphilic copolymers forms the hydrophobic core, which incorporates hydrophobic molecules, and the water-soluble block forms the hydrophilic shell to stabilize the micelles in aqueous media and, ideally, shield the core and drug from unfavorable interactions with the environment. To date, a large number of amphiphilic block copolymers have been utilized to prepare polymeric micelle taxanes formulations (Table S1).^[23–33] However, these formulations exhibit varied loading capacity ($LC = \text{weight of}$

drug/weight of excipients + drug). The majority of polymeric micelles showed low LC values of up to 10%^[24,25,27,29–32] with only a few copolymers/formulations showing higher LC of about 20–30%.^[23,26,28,33] Noticeably, some formulations exhibit a reasonable LC , but overall drug solubility may be rather low.^[34,35] Because drug solubilization in polymeric micelles is critically dependent on the drug interactions with the core forming hydrophobic block of the micelles,^[36] a significant redesign of this core appears to be needed to address the current challenges to solubilization of taxanes.

At the same time, there is also a need to reconsider the structure of the micelle shell. Notably, majority of investigators employ polyethylene glycol (PEG) as the hydrophilic and non-ionic component of the amphiphilic block copolymers to ensure stealth behavior and safety.^[37] At the same time, because of the extensive use of PEG-containing cosmetics and other body contact products, a considerable portion of human population bear antibodies against PEG.^[38,39] There is an increasing evidence and growing concern that antibody response against PEG can affect the efficacy of PEGylated drugs and drug nanoformulations in a subset of patients.^[38,39] This provides the rationale for selecting a different polymer chemistry platform for the design of the polymeric micelle corona.

One such platform, poly(2-oxazoline)s (POx), has attracted attention in different applications such as drug^[40] or protein carriers,^[41–43] antimicrobials,^[44] biocompatible coatings,^[45,46] hydrogels,^[47] tissue engineering scaffolds,^[48] gene delivery systems,^[49,50] as alternative to PEG.^[51,52] One interesting feature of POx is the possibility to fine-tune the hydrophilicity/hydrophobicity via variation of the side chain originating from the two-position and four-position of the monomer^[53] in the monomers. The water solubility decreases as the length of the side chain increases. Poly(2-methyl-2-oxazoline) (PMeOx), is highly hydrophilic, poly(2-ethyl-2-oxazoline) (PEtOx), and poly(2-propyl-2-oxazoline)s are amphiphilic and show a temperature-dependent water solubility.^[54–57] Poly(2-butyl-2-oxazoline)s (PBuOx) is the first non-water-soluble POx of the poly(*n*-alkyl-2-oxazoline) homologue series.^[56,58–60] Also, different architectures such as stars^[61] and brushes^[62–64] are readily accessible.

We have previously discovered taxane nanoformulations based on poly(2-oxazoline) polymeric micelles that display extremely high LC values (>40% w/w) and very high drug concentration (>40 g/l), have uniform particle size below 50 nm, and are very stable upon storage.^[65–67] Previous work was based on a triblock copolymer having PBuOx as the hydrophobic and PMeOx as the hydrophilic block. Herein, we present detailed studies on the preparation and characterization of micellar POx/taxane formulations, in which the chemical structure of the hydrophobic block was changed systematically. The aim of the study was to better understand pertinent structure property relationships by altering the composition of the block copolymer, the drug/POx ratio, and the drug and POx concentrations. We report on the physicochemical characteristics, such as micelle size and size distribution, *in vitro* stability, and *in vitro* cytotoxicity of the selected formulations in several cancer cell lines.

EXPERIMENTAL

Materials

All chemicals and materials were purchased from Sigma-Aldrich (Munich, Germany), Acros Organics (Geel, Belgium), and Fisher

Scientific Inc. (Fairlawn, NJ, USA). 2-Nonyl-2-oxazoline (NOx) was received as a gift from Henkel KGaA (Düsseldorf, Germany). For nuclear magnetic resonance (NMR) analysis, the deuterated solvents were obtained from Deutero GmbH (Kastellaun, Germany). Anticancer drugs were purchased from LC Laboratories (Woburn, MA, USA). The MCF-7 (HTB-22™), PC3 (CRL-1435™), and MDA-MB-231 (HTB-26™) cells were originally obtained from American Type Culture Collection. LCC-6 (wild type) and LCC-6-MDR (P-glycoprotein positive) cells were kindly donated by Dr. Ojima, Department of Chemistry and Institute of Chemical Biology and Drug Discovery, State University of New York at Stony Brook, NY.

Monomer synthesis

The general procedure for the monomer synthesis was carried out with modifications according to Witte and Seeliger *et al.*^[68] In brief, 1 eq of the nitrile, 1.2 eq of ethanolamine, and 0.025 eq cadmium acetate dihydrate were added to a nitrogen flushed flask and heated to 130°C. The reaction continued under reflux for 3–7 days until the reaction mixture turned dark brown. The raw product was dissolved in dichloromethane and purified by solvent extraction against a saturated NaHCO₃ solution (3×) and H₂O_{add} (1×). The organic phase was dried with MgSO₄, filtered, and concentrated under vacuum. The residue was mixed with CaH₂ and distilled via vacuum distillation. If necessary, the distillation was repeated, and the product stored under nitrogen atmosphere.

2-Sec-butyl-2-oxazoline (secBuOx)

bp = 95 °C (16 mbar), *n* (20°C) = 1.442.

¹H-NMR (CDCl₃, 300 K, and 500 MHz): δ [ppm] = 4.11 (t, 2H); 3.72 (t, 2H); 2.30 (sext, 1H); 1.58 (sept, 1H); 1.39 (sept, 1H); 1.07 (d, 3H); 0.82 (t, 3H).

2-Isobutyl-2-oxazoline (isoBuOx)

bp = 108°C (41 mbar), *n* (20°C) = 1.440.

¹H-NMR (ACN, 300 K, 500 MHz): δ [ppm] = 4.11 (t, 2H); 3.68 (t, 2H); 2.06 (d, 2H); 1.94 (ps-non, 1H); 0.91 (d, 6H).

2-Butyl-2-oxazoline (BuOx)

bp = 61°C (16 mbar).

¹H-NMR (CDCl₃, 300 K, 500 MHz): δ [ppm] = 4.10 (dt, 2H); 3.70 (t, 2H); 2.15 (t, 2H); 1.50 (ps-quin, 2H); 1.26 (ps-sext, 2H); 0.81 (t, 3H).

2-Isopentyl-2-oxazoline (isoPenOx)

bp = 65°C (23 mbar).

¹H-NMR (CDCl₃, 300 K, 500 MHz): δ [ppm] = 4.15 (t, 2H); 3.75 (t, 2H); 2.20 (ps-t, 2H); 1.57–1.44 (m, 3H); 0.85 (d, 6H).

2-Pentyl-2-oxazoline (PenOx)

bp = 90°C (30 mbar).

¹H-NMR (CDCl₃, 300 K, 500 MHz): δ [ppm] = 4.18 (t, 2H); 3.79 (t, 2H); 2.23 (t, 2H); 1.63–1.57 (m, 2H); 1.31–1.28 (m, 4H); 0.88–0.85 (m, 3H).

2-Heptyl-2-oxazoline (HepOx)

bp = 110°C (19 mbar).

¹H-NMR (CDCl₃, 300 K, 500 MHz): δ [ppm] = 4.21 (t, 2H), 3.81 (t, 2H), 2.26 (t, 2H); 1.62 (ps-quin, 2H); 1.32–1.27 (m, 8H); 0.87 (t, 3H).

2-Benzyl-2-oxazoline (BzOx)

bp = 100°C (5 mbar).

¹H-NMR (CDCl₃, 300 K, 500 MHz): δ [ppm] = 7.27 (m, 5H); 4.16 (t, 2H); 3.7 (t, 2H); 3.57 (s, 2H).

Polymerization

Amphiphilic diblock and triblock copolymers were synthesized by living cationic ring-opening polymerization as previously described.^[65] All substances used were refluxed over CaH₂ and distilled under nitrogen. The chemical structures, molar masses, dispersities, and critical micelle concentrations (CMC) of the synthesized polymers are summarized in Table 1.

Instrumental measurement

The NMR spectra were obtained using a Bruker DRX 500 P (¹H: 500.13 MHz) at room temperature (RT). The residual protonated solvent signals (ACN: 1.94 ppm, MeOH: 3.31 ppm, CHCl₃: 7.26 ppm) were used to calibrate the spectra. Gel permeation chromatography (GPC) was performed on a Polymer Laboratories GPC-120 (column setup: 1× PSS GRAM analytical 100, Polymer Standards Service, Mainz, Germany) with *N,N*-dimethyl acetamide as eluent (5 mmol/l LiBr, 1 wt% H₂O, 70°C, 1 ml/min) and poly(methyl methacrylate) standards. Microwave-supported polymerization was performed using a CEM Discover microwave.

Pyrene fluorescence measurements

Pyrene solutions (10 μl, 25 μM) in acetone were added to vials. After evaporation of acetone, 0.5 ml polymer solutions of various concentrations in deionized water were added to the probe. The samples, with a final concentration of pyrene of 5 × 10⁻⁷ M, were equilibrated for at least 3 h upon shaking at RT in the dark. The pyrene fluorescence spectra were recorded using a Fluorolog3 (HORIBA Jobin Yvon, Bensheim, Germany) spectrofluorometer (λ_{ex} = 333 nm, λ_{em} = 360–400 nm, slide width 1 nm, and step width 0.5 nm). The CMC is assumed where an increase in fluorescence intensity is observed. Also the ratio of the I₁ and I₃ band at the highest polymer concentration has been used to estimate the polarity of the micro-environment of the pyrene. No excimer band formation was observed.

Wilhelmy plate tensiometry

Polymer stock solution in DI water (1 g/l) was automatically added stepwise to 30 mL DI water to analyze the concentration range from 0.001 to 0.5 g/l via the tensiometer DCAT 11 (DataPhysics Instruments GmbH). The surface tension was measured after the added polymer solution was stirred for 5 s and equilibrated for 30 s.

Preparation of drug-loaded POx micelles

Drug-loaded POx micelles were prepared using the film hydration method.^[65] Pre-determined volumes of POx and drug stock solutions (each at 10 g/l in ethanol) were mixed well. Ethanol was removed by airflow at 40°C, and the formed thin film was further dried *in vacuo* to remove residual ethanol. Subsequently, the aqueous medium was added to the dried film, and the mixture was incubated at 45–50°C for diblock POx and 55–60°C for triblock POx for designated periods. The incubation time depended on the polymer and drug concentration. Specifically 5 min was

Table 1. Doubly amphiphilic tri- and di-block copoly(2-oxazoline)s used in this study

ID	Structure	Molar Mass (g/mol) NMR	Dispersity GPC	Critical Micelle Concentration (CMC) ^{a,b}	Maximum Solubilization of PTX (g/l) ^c
T1		10,000	1.1	1-5 μM ^a	9.6±0.9
T2		10,000	1.1	n.a.	3.6±0.2
T3		9,400	1.2	3 μM ^a 12 μM ^b	8.5±0.02
T4		9,200	1.1	24 μM ^a	8.3±0.9
T5		8,900	1.3	40 μM ^a 25 μM ^b	7.8±0.7
T6		8,700	1.2	n.a.	8.7±0.1
T7		8,500	1.1	10 μM ^a	3.2±0.4
T8		8,300	1.4	4.4 μM ^a	5.6±0.7
D1		7,100	1.2	2.5 μM ^b	2.0±0.1

^aas measured by surface tension method (Wilhelmy plate).

^bas measured by pyrene fluorescence probe.

^cas measured when polymer concentration was fixed as 10 g/l.

^ddetermined using MeOx₂₂-*b*-PenOx₁₆-*b*-MeOx₃₃

employed for low concentrations of polymer and drug (~10 g/l polymer; ~4 g/l drug) and 20 min for high concentration of polymer and drug (~50 g/l polymer; ~50 g/l drug). The mixture was cooled down to RT and centrifuged at 10,000 rpm (9630 × g) for 3 min (Sorvall Legend Micro 21R Centrifuge, Thermo Scientific) to remove potentially unloaded drug. The clear supernatant containing the drug-loaded polymeric micelles was used in subsequent experiments.

Analysis of drug loading in POx micelles

The amount of drug solubilized in POx micelles was quantified with an isocratic reverse-phase high-performance liquid chromatography (HPLC) system (Agilent Technologies 1200 Series, 250 mm × 4.6 mm Nucleosil C18 – 5 μm column). The drug-loaded micelles were diluted with mobile phase (ACN/water 55/45, v/v) and injected (20 μl) into the HPLC system. The flow rate was 1.0 ml/min and column temperature was 30°C. Detection wavelength was 227 nm. Retention time for paclitaxel and doxorubicin were 8.6 and 7.8 min, respectively.

Drug-loading calculations

The following equations were used to calculate the drug-loading capacity (*LC*) and loading efficiency (*LE*):

$$LC = \frac{m_{\text{drug}}}{m_{\text{drug}} + m_{\text{excipient}}} \cdot 100\% \quad (1)$$

$$LE = \frac{m_{\text{drug}}}{m_{\text{drug added}}} \cdot 100\% \quad (2)$$

where m_{drug} and $m_{\text{excipient}}$ are the weight amounts of the solubilized drug and polymer excipient in the solution, while $m_{\text{drug added}}$ is the weight amount of the drug added to the dispersion. Drug concentration (*DC*) was determined by HPLC and calculated against free PTX standards as described above and no loss of POx during micelles preparation was assumed.

Dynamic light scattering (DLS)

The size and size distribution of drug-loaded POx micelles was determined using DLS (Nano-ZS, Malvern Instruments Inc., UK). The drug-loaded micelles were diluted prior to the measurement with the respective aqueous medium to yield 1 g/l final polymer concentration. The intensity-mean z-averaged particle size (effective diameter) and the polydispersity index (PDI) were obtained from cumulant analysis performed by the supplier's software (Malvern Instruments Ltd, Malvern, UK) and were used to report the hydrodynamic diameters of drug-loaded POx micelles as size.

The stability studies of the triblock copolymer formulations in phosphate buffered saline (PBS) at maximum PTX loading were performed on an ALV/DLS/SLS-5000 compact goniometer system as described previously and analyzed accordingly.^[67]

POx micelles stability studies

The effects of aqueous media, storage temperature, lyophilization, redispersion and dilution on the stability of POx micelles were evaluated. Effect of dilution was studied with different dilution factors (×50–×500). For all experiments, following size measurements, micelles solutions were centrifuged at 10,000 rpm (9630 × g) for 3 min to remove the

precipitated drug. The remaining PTX amount in the micelles was quantified by HPLC as described above.

Cytotoxicity assay

The *in vitro* cytotoxicity of drug-loaded micelles was evaluated by the MTT assay. Briefly, cells were seeded at 5000 cells per well in 96-well plates 24 h prior to treatment with the drug. Cells were incubated with the micellar drug for 24 h; the incubation medium was replaced with the fresh medium, and cells were incubated for another 72 h. Subsequently, the medium was removed, and a 100 μl MTT solution (1 g/l in fresh medium) was added to each well. The cells were incubated for additional 3 h at 37°C, the medium was discarded, and a 100 μl dimethyl sulfoxide per well were added to dissolve the formed formazan salt. Absorbance at 562 nm was measured using a plate reader (SpectraMax M5, Molecular Devices, Sunnyvale, CA, USA). Cell survival rate was calculated as compared with untreated cells. Blank POx micelles and free taxane were used as negative and positive controls, respectively. Each concentration of the micellar formulation, blank POx micelles, and free taxane were tested separately in six wells. The 50% inhibition of cellular growth (IC_{50}) value was calculated using GraphPad Prism software (GraphPad Software, Inc., La Jolla, CA, USA). The data are presented in means ± standard error means (SEM).

RESULTS

Preparation and characterization of POx micellar taxanes formulations

The drug-loaded POx polymeric micelles were prepared by the film hydration method previously reported and illustrated in Fig. 1. The effects of (i) the structure of the POx copolymer; (ii) drug structure; and (iii) external parameter on solubilization capacity of POx and stability were evaluated. The solubilization capacity of POx was defined by loading capacity (*LC*, eqn 1), drug concentration (*DC*), loading efficiency (*LE*, eqn 2), and particles size and size distribution.

Effect of the POx structure on solubilization of PTX

The chemical structures, molar masses, and CMC of the polymers evaluated in this study are summarized in Table 1. For the triblock copolymers T1 to T7, the length of the hydrophobic middle block has been gradually decreased with increasing side chain length of the monomer in order to maintain the water solubility of the polymer. To compare the drug solubilization capacity of diblock and triblock copolymers, a diblock copolymer containing BuOx as the hydrophobic block was synthesized and evaluated (D1).

As recently discussed in detail,^[67] T1 and T7 represent opposite ends in terms of PTX loading. Here, we investigated the change in the properties of the polymeric micelles by gradually changing the flexibility and length of the side chain of the core-forming hydrophobic block (T2 to T6). The core polarity was determined by the I_1/I_3 ratio in the fluorescence spectra of pyrene using a well-known procedure.^[69] Using this method, we determined that the isoBuOx cores of T3 micelles ($I_1/I_3 = 1.75$) exhibited similar high polarity as BuOx cores in T1 micelles ($I_1/I_3 = 1.79$). As the length of the side chain increased, the polarity decreased. Thus, the PenOx and isoPenOx cores in T4 and T5 micelles were somewhat less polar ($I_1/I_3 = 1.66$ and $I_1/I_3 = 1.55$, respectively), while the NOx cores of T7 micelles were the least polar, according to the pyrene assay

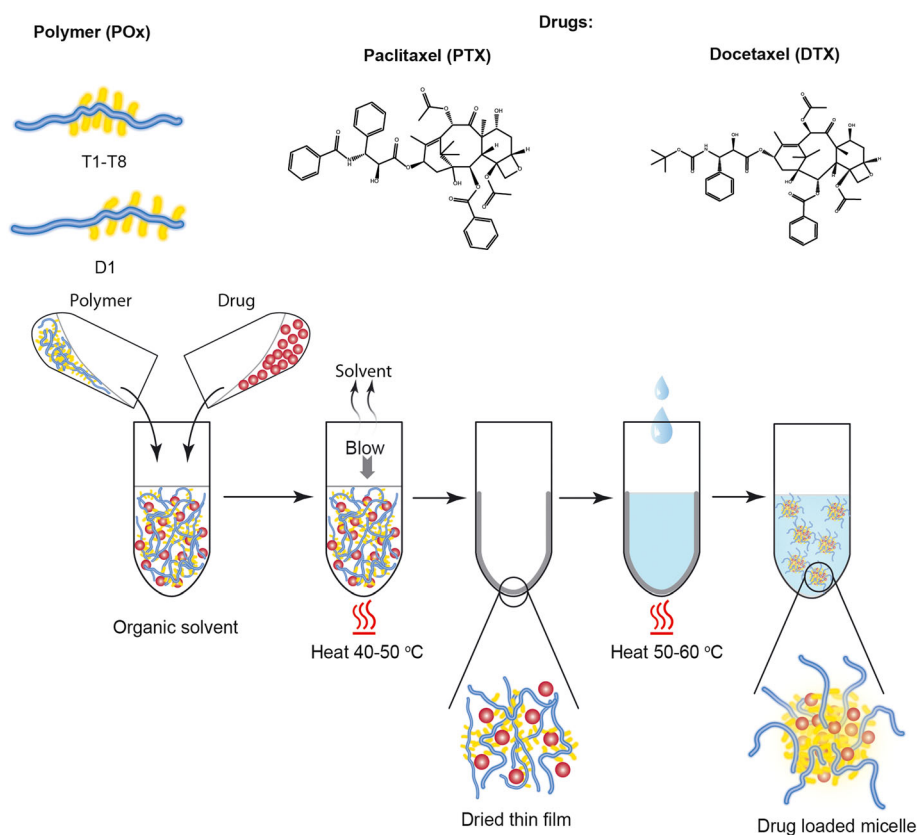


Figure 1. Schematic representation of the preparation of the drug-loaded poly(2-oxazolines) (POx) micelles. The drug loaded POx micelles were prepared by film hydration method involving (a) dissolution of the drug and block copolymer in a common solvent (e.g. ethanol), (b) solvent evaporation to form the film of the drug-solvent blend, and (c) hydration of the formed film and dispersion in water. This figure is available in colour online at wileyonlinelibrary.com/journal/pat

($I_1/I_3 = 1.28$). Interestingly, the observed dependency of the core polarity on the structure of the core-forming blocks is consistent with the data on the hydrophobicity of these blocks. Based on the measurements of the contact angles of the films made of the homopolymer analogs of the respective core-forming blocks, the hydrophobicity increased as the overall length of the side chain increased ($\text{secBuOx} < \text{isoBuOx} < \text{BuOx} \approx \text{isoPenOx} < \text{HeptOx}$) (Table S2). Interestingly, most triblock copolymer micelles in PBS, ranging from micelles having highly polar and weakly hydrophobic isoBuOx cores (T3) to those having the hydrophobic HepOx cores (T6), exhibited high PTX loadings. Only T2 and T7 micelles seemed to be either too polar or too hydrophobic for good PTX loading (Fig. 2).

These first studies were performed using rather low volumes of the PTX polymeric micelle formulations (0.1 ml). To study the stability of selected formulations (T1, T2, T4, T6, and T7), we needed to scale up to obtain sufficient volumes for DLS measurements with a goniometer. Scaling up to 1.5 ml did not seem to be an issue for T1 and T2, which retained their maximum LC values observed when the smaller volumes were studied. However, surprisingly, the scaling up led to a significant decrease in the apparent LC values for the copolymers with more hydrophobic blocks, T4, T6, and T7 to less than 30 wt% PTX. The issues with scaling up these PTX formulations are not clear at the moment. Perhaps, they involve crystallization of the polymers and/or the drug or incomplete solvent separation using the laboratory equipment.

The stability of the PTX-loaded POx micelles upon storage also depended on the structure of the core-forming block. As

previously reported, PTX-loaded T1 micelles in PBS were very stable and displayed no changes in the particle size and drug loading for at least 7 months.^[67] The second highest stability in comparison to the remaining triblock copolymers was exhibited by T7 micelles that were stable for about 1 month. With the exception of T1, the stability of the drug-loaded micelles increased as the core hydrophobicity increased. For example, at 30 wt% PTX loading, the T2 micelles with *sec*BuOx core precipitated after 1 day. At the comparable PTX loading (29 wt%), the T6 micelles with HepOx core were relatively stable and precipitated only after 9 days. Taken together, T2 having the least hydrophobic *sec*BuOx core-forming block appears to be the worst polymer for PTX solubilization of all studied POx block copolymers. In contrast, its close structural analog, T1, having a slightly more hydrophobic but polar BuOx core-forming block, is the best polymer to solubilize PTX. At this time, we are unable to explain the drastic differences between *sec*BuOx and BuOx cores.

To further investigate the T1-based formulations, the block copolymer and PTX “feed” concentrations set upon preparation of the micelle solutions were simultaneously varied at the constant T1/PTX weight ratio of 1:1. Interestingly, the LE and LC observed at the drug and copolymer concentrations of 5 g/l and below were less than those observed in the more concentrated systems (Fig. 3a). The formulations formed in this concentration range displayed relatively large z-averaged particle size (approx. 200 to 300 nm) and very large polydispersity (PDI approx. 0.6 to 0.9) (Fig. 3b). This suggests formation of either polymer-drug aggregates or suspended PTX crystals that could

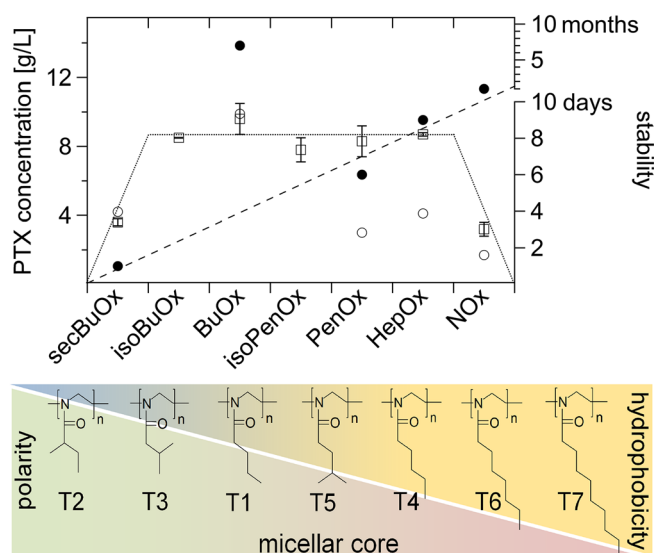


Figure 2. Effect of chemical composition of the hydrophobic block on the maximum paclitaxel (PTX) solubility observed with poly(2-oxazoline)s (POx) micelle formulations prepared at 0.1 ml scale (squares) and stability over time (filled circles) of POx micelle formulations prepared at 1.5 ml scale at different PTX concentration as shown in the figure (empty circles) in phosphate buffered saline at room temperature. Lines are added as a guidance for the eye and do not represent a fit. The stability study was carried out using multi-angle dynamic light scattering with a goniometer. Formation of large aggregates and/or precipitation was considered as end point. This figure is available in colour online at wileyonlinelibrary.com/journal/pat

not be separated by centrifugation. At higher concentrations, starting from 10 g/l and up to 50 g/l, the polymeric micelles exhibit very high *LE* (about 80%) and *LC* (about 44%). In

particular, at 50 g/l, the *DC* value (i.e. the actual solubilized PTX concentration measured in the micellar phase) was about 40 g/l (38.7 ± 2.6 g/l). Despite the very high PTX concentration, these micelles were small 28.6 ± 1.1 nm and quite uniform ($PDI = 0.14 \pm 0.013$). Overall, the observed behavior suggested very strong dependence of the physicochemical properties of PTX-loaded micelle systems on dilution. Notably, no significant changes in the z-averaged particle sizes of the unloaded T1 micelles were observed in the same concentration range (data not shown).

We also examined whether the solubilization of PTX can be further improved by introducing aromatic BzOx moieties in the hydrophobic core-forming block, along with BuOx, to enable additional interactions of this block with the aromatic residues of PTX. To this end, BzOx was copolymerized with BuOx (Table 1, T8). The effect of the change of the PTX concentration on the solubilization profile was evaluated while keeping the T8 concentration constant (10 g/l). Similar to previously reported results with T1 and T7,^[67] the *DC* and *LC* values initially linearly increased, and *LE* remained nearly constant as the PTX feed concentration increased (Fig. 4a). The maximum *LC* was observed at 6 g/l. Increasing the PTX feed concentration above this point was followed by a rapid decrease in both *LE* and *LC* values. At 10 g/l of PTX, *LC* and *LE* were under 2 wt%. Notably, the z-averaged particle size was under 50 nm, and the particle polydispersity was relatively low until the maximal loading was reached (Fig. 4b). Above this point, the z-averaged particle size rapidly increased to 100 nm, accompanied by an increase in *PDI* to approx. 0.5.

We also investigated the effect of simultaneous variation of T8 and PTX feed concentrations while keeping the POx/PTX weight ratio at 1:0.6 corresponding to the maximum *LC* for this system. In this experiment, the *LE* and *LC* values practically did not

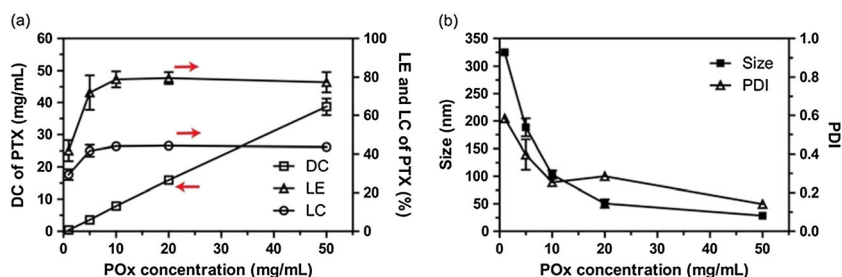


Figure 3. Effect of T1 and paclitaxel (PTX) feed concentrations at room temperature (RT) on the (a) solubilization of PTX in T1 micelles in DI water at RT as represented by drug concentration (*DC*), loading efficiency (*LE*), and loading capacity (*LC*) values and (b) z-averaged particle size and polydispersity index. T1 concentration was varied from 1 to 50 g/l at constant T1/PTX weight ratio of 1:1. Data are means \pm SD ($n = 3$). This figure is available in colour online at wileyonlinelibrary.com/journal/pat

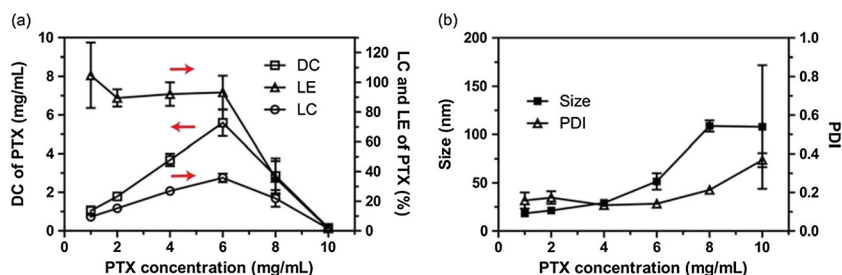


Figure 4. Effect of paclitaxel (PTX) feed concentration on the (a) solubilization of PTX in T8 micelles in DI water at room temperature as represented by drug concentration (*DC*), loading efficiency (*LE*), and loading capacity (*LC*) values and (b) z-averaged particle size and polydispersity index. Concentration of T8 was set to 10 g/l and PTX concentration was varied from 1 to 10 g/l. Data are means \pm SD ($n = 3$). This figure is available in colour online at wileyonlinelibrary.com/journal/pat

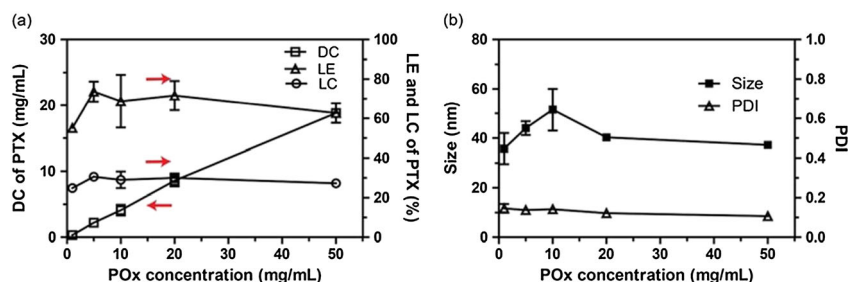


Figure 5. Effect of T8 and paclitaxel (PTX) feed concentrations on the (a) solubilization of PTX in T8 micelles in DI water at room temperature as represented by drug concentration (DC), loading efficiency (LE), and loading capacity (LC) values and (b) z-averaged particle size and polydispersity index. T8 concentration was varied from 1 to 50 g/l at constant poly(2-oxazoline)s (POx)/PTX weight ratio of 1:0.6. Data are means \pm SD ($n = 3$). This figure is available in colour online at wileyonlinelibrary.com/journal/pat

change and remained approx. 70% and 30%, respectively in the entire concentration range (Fig. 5a). There was a small increase in the z-averaged particle size with the maximal value (51.6 ± 8.5 nm) observed at 10 g/l T8 and 6 g/l PTX. At higher concentrations of the copolymer and drug, the particle size decreased and appeared to level off at approx. 40 nm (Fig. 5b).

The solubilization of PTX using diblock copolymer D1 was less effective compared with the respective triblock copolymer T1 (Fig. 6). When the PTX feed concentration was varied while keeping the D1 concentration constant (10 g/l), the maximum LC value (16.3 ± 0.4 wt%) was observed at 2 g/l PTX. Under this condition, the incorporation of the drug in the micelles was nearly complete ($LE 97.9 \pm 2.5\%$). At higher PTX feed concentrations, e.g. at 4 g/l PTX, all solubilization parameters (DC, LE, and LC) rapidly decreased with the LC and LE being as low as 3.36 ± 0.9 wt% and 11.8 ± 3.0 %, respectively. The decrease in DC, LC, and LE was accompanied by an increase in the z-averaged

particle size. Notably, according to DLS measurements, in the absence of PTX, D1 in DI water forms two types of particles—one small with size around 22 nm and another large with sizes of 90 to 100 nm. The transmission electron microscopy images of negatively stained D1 particles are consistent with DLS results as both spherical micelles of 10 to 20 nm and worm-like micelles with the major axis length of 100–200 nm and aggregates with diameters of 100–200 nm are observed under these conditions (Fig. S1). Based on that, we suggest that a relatively high PDI (0.55 ± 0.13) observed at 1 g/l PTX feed concentration might be due to heterogeneous morphologies of the D1 polymeric micelles. A rapid decrease of PDI at 2 g/l PTX feed concentration probably corresponds to a morphology transition from heterogeneous mix of different micelles to homogeneous spherical micelles, which would be consistent with previous report of the polymeric micelle morphology switch upon increasing PTX loading observed for T1.^[67]

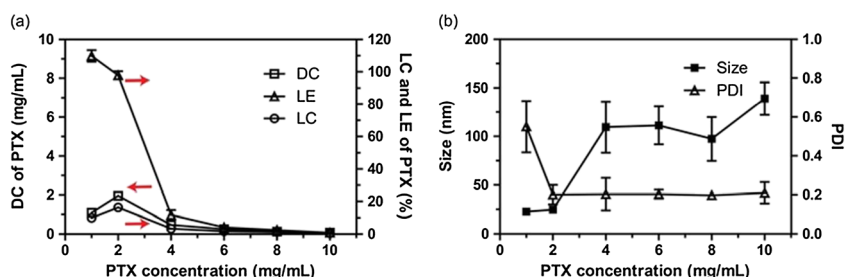


Figure 6. Effect of paclitaxel (PTX) feed concentration on the (a) solubilization of PTX in D1 micelles in DI water at a room temperature as represented by drug concentration (DC), loading efficiency (LE), and loading capacity (LC) values and (b) z-averaged particle size and polydispersity index. Concentration of D1 was set at 10 g/l and PTX concentration was varied from 1 to 10 g/l. Data are means \pm SD ($n = 3$). This figure is available in colour online at wileyonlinelibrary.com/journal/pat

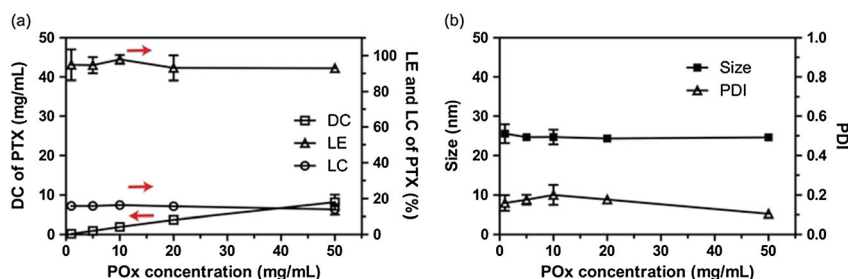


Figure 7. Effect of D1 and paclitaxel (PTX) feed concentrations on the (a) solubilization of PTX in D1 micelles in DI water at RT as represented by drug concentration (DC), loading efficiency (LE), and loading capacity (LC) values and (b) z-averaged particle size and polydispersity index. D1 concentration was varied from 1 to 50 g/l at constant poly(2-oxazoline)s (POx)/PTX weight ratio of 1:0.2. Data are means \pm SD ($n = 3$). This figure is available in colour online at wileyonlinelibrary.com/journal/pat

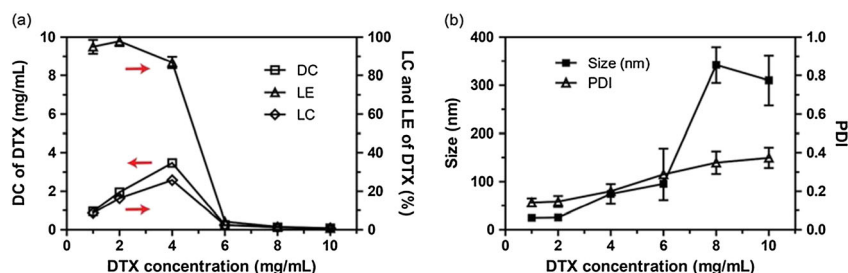


Figure 8. Effect of docetaxel (DTX) feed concentration on the (a) solubilization of DTX in D1 micelles in DI water at room temperature as represented by drug concentration (DC), loading efficiency (LE), and loading capacity (LC) values and (b) z-averaged particle size and polydispersity index. Concentration of D1 was set at 10 g/l and DTX concentration was varied from 1 to 10 g/l. Data are means \pm SD ($n = 3$). This figure is available in colour online at wileyonlinelibrary.com/journal/pat

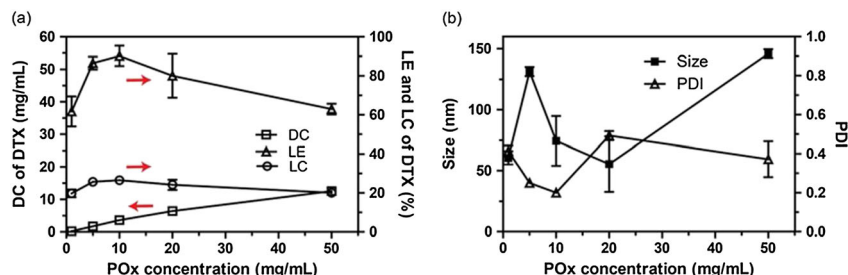


Figure 9. Effect of D1 and docetaxel (DTX) feed concentrations on the (a) solubilization of DTX in D1 micelles in DI water at room temperature as represented by drug concentration (DC), loading efficiency (LE), and loading capacity (LC) values and (b) z-averaged particle size and polydispersity index. D1 concentration was varied from 1 to 50 g/l at constant poly(2-oxazolines) (POx)/PTX weight ratio of 1:0.4. Data are means \pm SD ($n = 3$). This figure is available in colour online at wileyonlinelibrary.com/journal/pat

In the final experiment described in this section, both D1 and PTX feed concentrations were simultaneously increased while keeping the POx/PTX weight ratio at 1:0.2. In this case, the POx micelles displayed LE values of about 90%, and the DC linearly increased, while the LC remained practically constant (Fig. 7a). The z-averaged particle size also remained unchanged (approx. 25 nm) while the PDI was under 0.2 and decreased to 0.1 as the D1 concentration reached 50 g/l (Fig. 7b).

Effect of the taxane structure on solubilization: DTX versus PTX

Effect of structure of taxanes on their solubilization using various POx block copolymers was evaluated using DTX. DTX is a close structural analogue of PTX, in which a phenyl group is substituted with a *tert*-butanol moiety. While T1 and T8 polymeric micelle formulations of DTX exhibited almost no differences to analogous formulations of PTX in terms of LE, LC, size, and PDI (Fig. S2–S5), the diblock copolymer, D1, performed much better with DTX than with PTX.

For example, the maximum solubilization of DTX in the D1 micelles (10 g/l D1) was observed at 4 g/l DTX, which is twice as much as the corresponding feed concentration of PTX. The LE value in this D1-DTX system was 86.78 ± 2.98 %, which corresponded to LC of 25.76 ± 0.66 % (Fig. 8a). The latter value again was considerably higher compared with the LC values observed in D1 micelles with PTX. At 6 g/l DTX feed concentration, LE and LC values decreased to 4.18 ± 0.66 % and 2.45 ± 0.38 %, respectively and then further decreased as the DTX feed concentration was elevated. Under these conditions along with the drastic decrease in the drug solubilization, the formation of aggregates was observed (Fig. 8b). Thus, the z-averaged particle size increased from 75 nm at 4 g/l DTX to 310 nm at 10 g/l

DTX. However, in contrast to the D1-PTX formulation, the PDI values increased as well suggesting formation of the heterogeneous aggregates with the particle size ranging from 200 to 300 nm. Also, no more small micelles could be observed at 8 and 10 g/l DTX.

When the weight ratio of POx to DTX was kept constant at 1:0.4, the maximum LC value was obtained at 10 g/l of D1 (25.76 ± 0.66 wt%), and overall LC value remained above 20% in the entire range of the polymer concentrations (Fig. 9a). However, the particle size distribution was quite broad with little if any small polymeric micelles observed at 1, 20, and 50 g/l. At 5 and 10 g/l, no such micelles could be detected by DLS, and most particles appeared to represent aggregates between 120 and 200 nm (Fig. 9b). Overall, it appears that in contrast to the T1 triblock copolymers, the small micelles under 50 nm are not the preferred morphology for DTX incorporation in D1 systems. It remains to be determined if the large aggregates feature a different structured morphology, e.g. worm-like micelles, which can solubilize such elevated amounts of DTX.

Influence of environmental parameters on the stability of POx micelle formulations of taxanes

The stability of polymeric micelle formulations of drugs towards external challenges such as salt concentration and temperature is an important factor for storage and application of these formulations in clinic. Hence, the particle size and PDI over time of concentrated T1 (50 g/l) formulations of PTX and DTX (PTX 38.7 g/l or DTX 40.6 g/l in dispersed system) was investigated to determine their stability in various dispersion media, after lyophilization and upon dilution.

In contrast to the previously reported outstanding stability of the 10 g/l T1-PTX formulation in PBS over 7 months, we

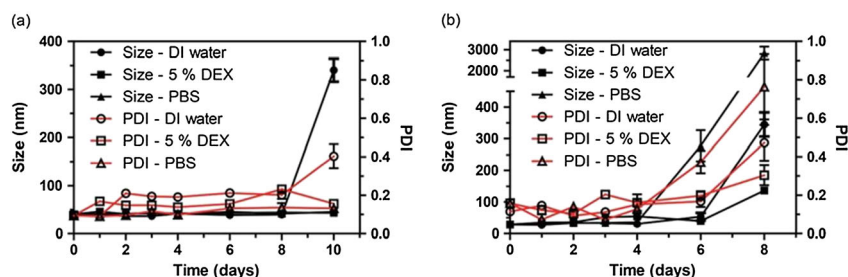


Figure 10. Stability of 50 g/l T1 micelle formulations of (a) paclitaxel (39.7 g/l) and (b) docetaxel (40.6 g/l) in DI water, 5% dextrose solution (DEX) or phosphate buffered saline at room temperature. This figure is available in colour online at wileyonlinelibrary.com/journal/pat

discovered that several formulations in DI water formed aggregates after just few days of observation. In particular, the highly concentrated 50 g/l T1-PTX formulation in DI water formed aggregates with effective diameters above 300 nm and broad polydispersity (PDI = 0.4) at day 10 (Fig. 10a). However, the very same formulation in PBS, and in 5% dextrose solution remained stable for 10 days. At the same time, the DTX-loaded micelles exhibited low stability not only in DI water, but also in PBS and 5% dextrose solution. Thus, the T1-DTX formulation in PBS was stable only for the first 4 days, and at day 6 exhibited a marked increase in the z-averaged particle size and PDI to 279.9 ± 49.2 and 0.37 ± 0.06 nm, respectively (Fig. 10b). At day 8, similar aggregation was observed for this formulation both in DI water and 5% dextrose solution.

We further assessed the stability of the formulations upon storage at lower temperature. Cooling of the T1-PTX and the T1-DTX formulations to 4°C had little if any effect on the particle size and polydispersity as well as on the LC values when compared with these formulations at RT (Fig. S6). Moreover, there was no change in the particle size, PDI, and LC upon storage of these formulations both at 4°C and RT for up to 3 days (Fig. S6). Notably, the formulations with very high drug content, such as 50 g/l T1-PTX formulation at PTX feed concentration 50 g/l could be lyophilized after preparation and re-dispersed in either DI water or PBS resulting z-averaged particle size and PDI being very similar to the original formulations (Table S3). Moreover, the reconstituted formulations exhibited good stability in DI water or PBS for at least 2 days.

If applied intravenously, any formulation will be diluted rapidly and drastically. Although an *in vitro* dilution cannot mimic dilution after injection in the complexity of potential effects, we were also interested in the behavior of the formulations upon dilution in aqueous media. Considering that a patient might receive about 400 mg PTX in a standard treatment, injecting 10 ml of our current formulation might suffice to apply this dose. With a rough estimate of 5 l of blood volume in an adult, a dilution factor of 500 can be estimated. To assess the potential effect of such dilution, we prepared the 50 g/l T1-PTX formulations at PTX feed concentration 50 g/l in DI water, 10 mM NaCl solution and PBS and diluted them to 50, 100, 200, 400, and 500-fold (Fig. S7 and S8). Interestingly, all formulations, including the formulation in DI water, displayed nearly constant particle sizes (approx. 50 nm) up to a 400-fold dilution (Fig. S8a–d). Moreover, the particle sizes remained practically unchanged for 2 weeks at RT. Notably, the formulation in DI water displayed higher polydispersity compared with formulations in 10 mM NaCl or PBS that more uniform up to 200-fold dilution. At greater dilutions,

all formulations became generally more polydisperse, and the PDI values increased over time especially at 500-fold dilution (Fig. S8d and f). At this maximal dilution, the formulation in DI water displayed an onset of aggregation on day 9, while the formulations in 10 mM NaCl or PBS still remained stable (Fig. S8e). Along with the particle size and polydispersity, we also measured the PTX content over time. To ensure removal of any precipitate, the samples were centrifuged, and the PTX content in the remaining micelle solutions was determined. All formulations retained solubilized PTX up to 400-fold dilution. Only at 500-fold dilution the PTX content decreased down to $47.29 \pm 7.67\%$ of the initial in DI water and $63.55 \pm 4.71\%$ of the initial in PBS because of the drug precipitation (Fig. S9).

In vitro cytotoxicity

The *in vitro* cytotoxicity of the 50 g/l T1 micelles loaded with PTX or DTX (both drugs at feed concentration 50 g/l) was determined in MCF-7, MDA-MB-231, and PC3 cancer cells (Fig. 11). The polymer alone showed no noticeable toxicity up to the highest concentration used in the formulations^[70] (data not shown).

In all cell models studied, with one exception described in the succeeding discussions, there was little if any difference in the cytotoxicity of the free drug and the polymer micelle-incorporated drug. Thus, the IC₅₀ values of free PTX in MCF-7, MDA-MB-231, and PC3 cancer cells were 2.0 ± 0.40 , 0.47 ± 0.12 , and 0.62 ± 0.36 nM, respectively (Table S4). The T1 micelle-incorporated PTX showed comparable cytotoxicity with IC₅₀ values of 1.5 ± 0.57, 0.39 ± 0.13, and 0.37 ± 0.08 nM, respectively. Likewise, the free DTX and T1 micelle DTX exhibited very similar cytotoxicity, in all but one cancer cell lines. The only exception was the MCF-7 cell line, for which the micellar DTX showed a somewhat higher IC₅₀ compared with the free drug.

Finally, we evaluated the effect of the block copolymer structure (T1, T8, and D1) on the cytotoxicity of the polymeric micelle formulations of PTX prepared at feed concentrations of 10 g/l POx and 2 g/l PTX (maximal loading ratio for D1) (Fig. 12). In this case, the cytotoxicity of the formulations was determined in MCF-7, MDA-MB-231, PC3, LCC-6, and the P-glycoprotein (P-gp) overexpressing multidrug resistant LCC-6-MDR cancer cell lines. All PTX formulations exhibited comparable cytotoxicity without significant differences observed between different block copolymer structures. Notably, all drug formulations produced significant cytotoxicity in the MDR cell line with IC₅₀ values being in the nM range, although these values were higher than those determined using the drug sensitive LCC-6-MDR cells (Table S5).

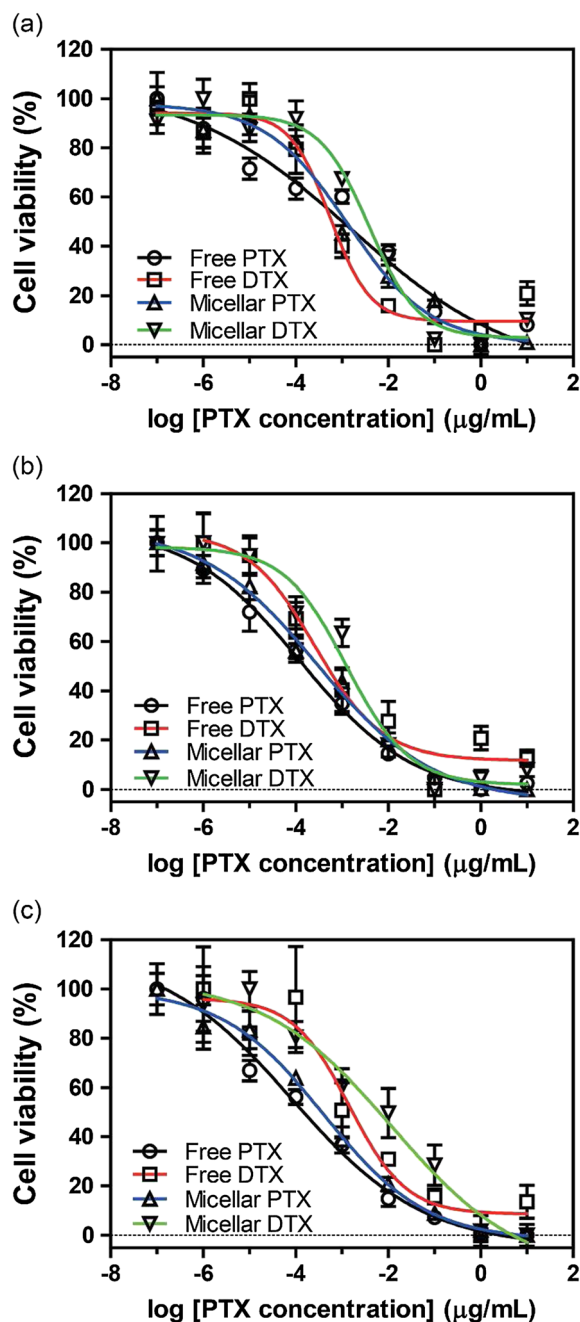


Figure 11. Dose-dependent cytotoxicity of T1-PTX micelles, T1-DTX micelles, free PTX, and free DTX in (a) MCF-7, (b) MDA-MB-231, and (c) PC3 cancer cells. The T1 micelle formulations were prepared at 50 g/l T1 and 50 g/l feed concentration of the drugs. Data are mean \pm SEM ($n=6$) for every drug concentration. PTX, paclitaxel; DTX, docetaxel. This figure is available in colour online at wileyonlinelibrary.com/journal/pat

DISCUSSION

Recent studies have shown that polymeric micelles composed of PMeOx-PBuOx-PMeOx triblock copolymers have very high capacity for solubilization of PTX, DTX, several third-generation Taxoids, and several other drugs and multiple drug combinations.^[65,66,71] The drug-loaded micelles could be easily prepared by the thin film hydration method.^[65] The exceptional solubilization capacity for taxanes appears to be unique to date for POx

amphiphiles and is attributed to the unusual micellar microenvironment of BuOx core forming block,^[65] which contains both hydrophobic and polar groups allowing dipole-dipole interactions or formation of H-bonds with the drug. It should be noted, however, that as of today, we were unable to find experimental evidence for H-bonding between the polymer and the drug, which still remains hypothetical.

Here, we report on a more detailed investigation of a small variation of triblock copolymer structure, in which hydrophobic blocks were gradually altered in terms of hydrophobicity and polarity. Surprisingly, relatively minor changes of the structure of the core-forming block, such as replacing BuOx with *sec*BuOx, were shown to decrease the solubilization capacity and/or stability of the formulations. Also, the addition of a small fraction of benzyl moieties to the BuOx block reduced the maximum loading capacity by almost a half. Furthermore, a diblock copolymer comprising a BuOx block displayed a significantly lower solubilization capacity with respect to PTX than the corresponding triblock copolymer with the similar length BuOx block. Thus, the balanced properties of the BuOx block and the polymer architecture in PMeOx-PBuOx-PMeOx are the reasons for the high drug loading, good reproducibility and stability of the polymeric micelles under various conditions. Moreover, relatively minor changes in the drug structure between PTX and DTX can also drastically affect the solubilization behavior. Thus, DTX has shown much better incorporation in the diblock copolymer micelles compared with PTX. Overall, this highlights the serendipitous character of our original finding of high drug-loading polymeric micelles formed by PMeOx-PBuOx-PMeOx triblock copolymers.

Other drug delivery systems with relatively high capacity for PTX have been also reported, although no formulation is known to have such an unprecedented high capacity as some of the triblock copolymer formulations described in this work (Table S1). Moreover, in contrast to the concentrated T1-PTX micelles that display small particle sizes at the maximum loading, other known polymeric micelle formulations of taxanes feature relatively large particle sizes. For example, the particle size of poly (IPAAm-co-AAm)-b-PDLLA micelles having a relatively high LC of 21.3% with respect to DTX was about 80 nm.^[28] The PEG_{5k}-CA₈ micellar PTX formulation had the LC of 25.9% for PTX and exhibited the particle sizes of about 90 nm.^[33] While such dimension particles are considered likely to penetrate and deliver treatment to permeable tumors, they are probably too large for the treatment of relatively impermeable tumors and distal metastases. As a result, to achieve better penetration into tumors, the polymeric micelles with particle sizes below 50 nm, even those having lower drug content, are given preference despite increased risk of the side effects associated with the potential toxicity of the excess of the polymeric carrier.^[22,72]

Here, we demonstrate that the POx/taxane formulations offer what seems to be an ideal way to combine high drug content while retaining the small size of the micelles below 50 nm. When the concentration of POx was increased from 10 to 50 g/l at constant POx/drug weight ratio, the high solubilization capacity of the PMeOx-PBuOx-PMeOx micelles was preserved (44–45% LC for both taxanes). Interestingly, in contrast to previous work, in which the PTX formulation was stable for over half a year in PBS at 10 g/l, the highly loaded and more concentrated formulation of PTX (approx. 50 g/l) was stable for only 8 days in DI water. The free tertiary and secondary amine groups of the piperazine end group should be essentially fully protonated at neutral pH

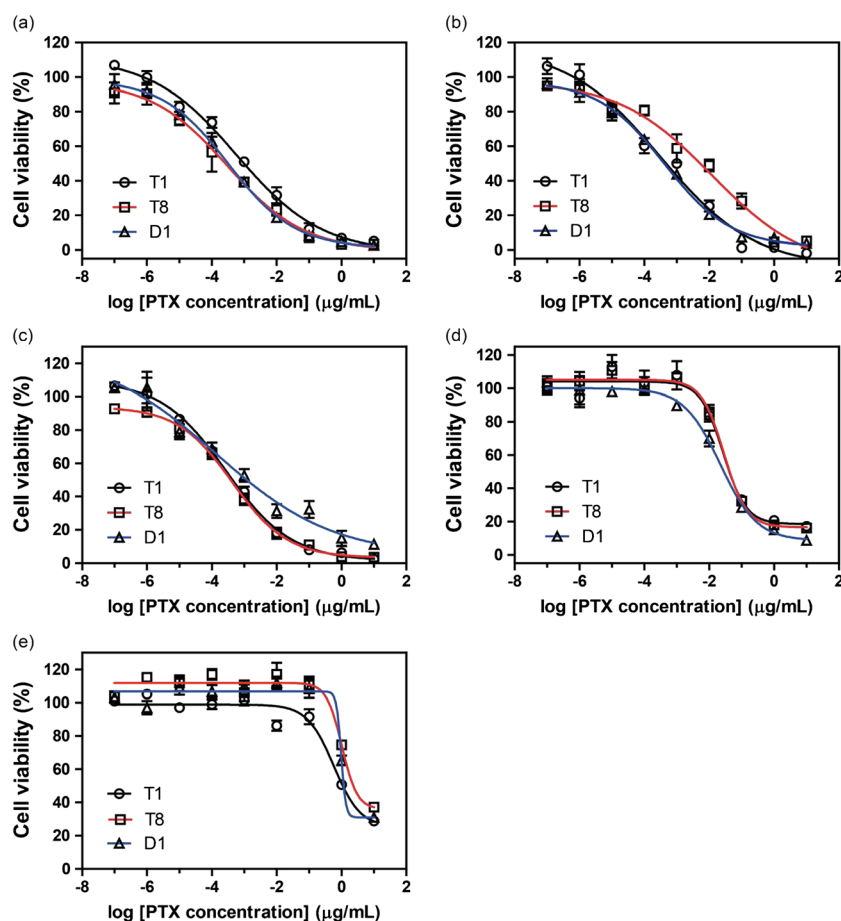


Figure 12. Dose-dependent cytotoxicity of poly(2-oxazoline)s (POx) micelle formulations of paclitaxel (PTX) in (a) MCF-7, (b) MDA-MB-231, (c) PC3, (d) LCC-6-WT, and (e) LCC-6-MDR cancer cells. The POx/PTX formulations were prepared at 10 g/l POx (T1, T8, and D1) and 2 g/l feed concentration of the PTX. Data are mean \pm SEM ($n = 6$) for every drug concentration. This figure is available in colour online at wileyonlinelibrary.com/journal/pat

which leads to slightly positive surface charge of the micelles (ζ -potential of T1 micelles = $+11.7 \pm 0.6$ mV). This may lead to a dependence of the micellization and solubilization behavior on the concentration and chemical nature of the small molecular mass electrolytes. Interestingly, no aggregation was observed in 5% dextrose solution for at least 10 days. T1 also showed excellent solubilization capacity for DTX, a structural analog of PTX. However, the formulation stability was quite distinct. The 50 g/l T1 micelles highly loaded with DTX (feed concentration of DTX 50 g/l) were much less stable than similar formulations of PTX independent of the used solvent (PBS, 5% dextrose or DI water). After 8 days, aggregation was observed in all three formulations. This is very interesting, because similar T1 micelles loaded with the DTX derivative SB-T-1214 (50 g/l T1 and 40 g/l SB-T-1214 in USP saline) did not show any change in size or PDI after 10 days.^[71] Nonetheless, all formulations were stable up to 6 days irrespective of the solvent and taxane derivative used. This is still remarkable considering the known propensity of taxanes for crystallization.

Moreover, the characteristics did not change upon lyophilization of the formulations. No cryoprotectants, often necessary for lyophilization, were required. Simple addition of DI water or other aqueous media to the lyophilized powders reconstituted the formulations, which were then stable for days. In addition, the concentrated formulations could be diluted in large volume (about 400 times) without significant size change. These results

demonstrate that the formulations fulfill basic criteria for the application in clinic. For instance, the concentrated drug formulations can be stored as lyophilized powder, simply re-dispersed in a suitable aqueous media for injection, and diluted to the desired concentration for intravenous (i.v.) administration. Leftovers of prepared formulations may be stored for further use for several days.

The POx micelle formulations of taxanes elicit cytotoxicity in a variety of cancer cell lines similar to free taxanes. We observed a trend for somewhat higher IC_{50} values for micellar drugs as compared with free drugs, which may be due to the delayed release of the drug from the micelles. However, the differences in most cases were not statistically significant. The IC_{50} values of micellar drugs tested in MDR cancer cell line were statistically higher than IC_{50} values of the micellar drugs in the sensitive cancer cell counterparts. It appears that the tested POx amphiphiles are unable to inhibit P-glycoprotein as some members of the Pluronics family do. This is interesting to note, because Pluronics known to inhibit P-glycoprotein have a similar hydrophilic/lipophilic balance as the presently tested POx-based amphiphiles.^[73,74]

In addition to the high solubilization capacity for taxanes, another advantage of POx is their low-toxicity. The acute oral LD_{50} (rats) and acute percutaneous absorption LD_{50} (rabbit) of PETox were over 4 g/kg, respectively.^[75] The i.v. administrations of 2 g/kg or repeated 50 mg/kg PETox into rats did not cause

any toxic and adverse effects.^[76] PMeOx and PEtOx homopolymers of low molar mass showed a fast distribution throughout the entire organism (mice) and a very rapid renal excretion.^[59] Also, POx-rotigotine conjugates have been very favorably tested in various species, including non-human primates.^[40,77] Consequently, we posit that POx are an excellent candidates to reduce or eliminate the excipients-induced side effects of current clinical formulation, including but not limited to taxanes. Compared with other micellar formulations in development, the significantly reduced amount of excipient needed, POx may abate the burden of excipients excretion and the risk of excipient accumulation upon sub-chronic or chronic exposure.

CONCLUSIONS

In conclusion, drug content, size, and stability of the formulations are highly dependent on the polymer structure (triblock/diblock and nature of hydrophobic block), chemical structure of the drug, and the ratio of drug to POx and POx concentration. Solubilization capacity for taxanes was generally found invariant to increasing concentrations of POx and PTX at the maximum LC for a given POx. So far, the triblock POx amphiphile with a BuOx middle block remains the best choice to formulate taxanes exhibiting the best stability in combination with high drug content (44–45 wt.% LC), small size (<50 nm), and overall concentration of taxane (\approx 40 g/l). The formulations showed similar cytotoxicity as free drugs in a variety of cancer cell lines and relatively high IC₅₀ values in MDR cancer cells. Taken the excellent solubilization capacity, stability, and *in vitro* activity, POx micelles show great potential as highly efficient drug delivery platform for taxanes and potentially other hydrophobic drugs.

Acknowledgement

Y.C.Han is grateful to the China Scholarship Council (CSC) for a postdoctoral fellowship and the support of PCSIRT.

REFERENCES

- [1] L. M. Zasadil, K. A. Andersen, D. Yeum, G. B. Rocque, L. G. Wilke, A. J. Tevaarwerk, R. T. Raines, M. E. Burkard, B. A. Weaver, *Sci. Transl. Med.* **2014**, *6*, 229ra43, 1–10.
- [2] P. B. Schiff, J. Fant, S. B. Horwitz, *Nature* **1979**, *277*, 665.
- [3] K. L. Hennenfent, R. Govindan, *Ann. Oncol.* **2006**, *17*, 735.
- [4] L. B. Michaud, V. Valero, G. N. Hortobagyi, *Drug Saf.* **2000**, *23*, 401.
- [5] A. C. Wolff, R. C. Donehower, M. K. Carducci, M. A. Carducci, J. R. Brahmer, Y. Zabelina, M. O. Bradley, F. H. Anthony, C. S. Swindell, P. A. Witman, *Clin. Cancer Res.* **2003**, *9*, 3589.
- [6] S. Spigel, S. Jones, F. Greco, J. Hainsworth, N. Dickson, N. Willcutt, S. Calvert, J. Pratt, *Proc. Am. Soc. Clin. Oncol.* **2002**, *21*, 406 (Abstr).
- [7] A. Cabanes, K. Briggs, P. Gokhale, J. Treat, A. Rahman, *Int. J. Oncol.* **1998**, *12*, 1035.
- [8] X. Zhang, H. M. Burt, G. Mangold, D. Dexter, D. Von Hoff, L. Mayer, W. L. Hunter, *Anticancer Drugs* **1997**, *8*, 696.
- [9] N. K. Ibrahim, N. Desai, S. Legha, P. Soon-Shiong, R. L. Theriault, E. Rivera, B. Esmali, S. E. Ring, A. Bedikian, G. N. Hortobagyi, J. A. Ellerhorst, *Clin. Cancer Res.* **2002**, *8*, 1038.
- [10] S. C. Kim, D. W. Kim, Y. H. Shim, J. S. Bang, H. S. Oh, S. W. Kim, M. H. Seo, *J. Control. Release* **2001**, *72*, 191.
- [11] T.-Y. Kim, D.-W. Kim, J.-Y. Chung, S. G. Shin, S.-C. Kim, D. S. Heo, N. K. Kim, Y.-J. Bang, *Clin. Cancer Res.* **2004**, *10*, 3708.
- [12] X. Zhang, H. M. Burt, D. Von Hoff, D. Dexter, G. Mangold, D. Degen, A. M. Oktaba, W. L. Hunter, *Cancer Chemoth. Pharm.* **1997**, *40*, 81.
- [13] A. Sparreboom, C. D. Scripture, V. Trieu, P. J. Williams, T. De, A. Yang, B. Beals, W. D. Figg, M. Hawkins, N. Desai, *Clin. Cancer Res.* **2005**, *11*, 4136.
- [14] H. S. Rugo, W. T. Barry, A. Moreno-Aspitia, A. P. Lyss, C. Cirrincione, E. L. Mayer, M. Naughton, R. M. Layman, L. A. Carey, R. A. Somer, *J. Clin. Oncol.* **2012**, *30*.
- [15] Y. Boucher, L. T. Baxter, R. K. Jain, *Cancer Res.* **1990**, *50*, 4478.
- [16] Y. Boucher, R. K. Jain, *Cancer Res.* **1992**, *52*, 5110.
- [17] M. H. Branton, J. B. Kopp, *Microb. Infect.* **1999**, *1*, 1349.
- [18] E. Brown, T. McKee, *Nat. Med.* **2003**, *9*, 796.
- [19] B. Diop-Frimpong, V. P. Chauhan, S. Krane, Y. Boucher, R. K. Jain, *Proc. Natl. Acad. Sci. U. S. A.* **2011**, *108*, 2909.
- [20] T. Stylianopoulos, C. Wong, M. G. Bawendi, R. K. Jain, D. Fukumura, *Meth. Enzymol.* **2012**, *508*, 109.
- [21] F. Yuan, M. Leunig, S. K. Huang, D. A. Berk, D. Papahadjopoulos, R. K. Jain, *Cancer Res.* **1994**, *54*, 3352.
- [22] H. Cabral, Y. Matsumoto, K. Mizuno, Q. Chen, M. Murakami, M. Kimura, Y. Terada, M. Kano, K. Miyazono, M. Uesaka, *Nat. Nanotechnol.* **2011**, *6*, 815.
- [23] M. G. Carstens, P. H. de Jong, C. F. van Nostrum, J. Kemmink, R. Verrijck, L. G. De Leede, D. J. Crommelin, W. E. Hennink, *Eur. J. Pharm. Biopharm.* **2008**, *68*, 596.
- [24] S. C. Lee, C. Kim, I. C. Kwon, H. Chung, S. Y. Jeong, *J. Control. Release* **2003**, *89*, 437.
- [25] M. Elsbahy, M.-È. Perron, N. Bertrand, G.-e. Yu, J.-C. Leroux, *Biomacromolecules* **2007**, *8*, 2250.
- [26] T. Hamaguchi, Y. Matsumura, M. Suzuki, K. Shimizu, R. Goda, I. Nakamura, I. Nakatomi, M. Yokoyama, K. Kataoka, T. Kakizoe, *Br. J. Cancer* **2005**, *92*, 1240.
- [27] D. Le Garrec, S. Gori, L. Luo, D. Lessard, D. C. Smith, M.-A. Yessine, M. Ranger, J.-C. Leroux, *J. Control. Release* **2004**, *99*, 83.
- [28] B. Liu, M. Yang, R. Li, Y. Ding, X. Qian, L. Yu, X. Jiang, *Eur. J. Pharm. Biopharm.* **2008**, *69*, 527.
- [29] L. Ostacolo, M. Marra, F. Ungaro, S. Zappavigna, G. Maglio, F. Quaglia, A. Abbruzzese, M. Caraglia, *J. Control. Release* **2010**, *148*, 255.
- [30] H.-C. Shin, A. W. Alani, D. A. Rao, N. C. Rockich, G. S. Kwon, *J. Control. Release* **2009**, *140*, 294.
- [31] X. Shuai, T. Merdan, A. K. Schaper, F. Xi, T. Kissel, *Bioconjug. Chem.* **2004**, *15*, 441.
- [32] O. Soga, C. F. van Nostrum, F. Marcel, C. J. F. Rijcken, R. M. Schifferers, G. Storm, W. E. Hennink, *J. Control. Release* **2005**, *103*, 341.
- [33] K. Xiao, J. Luo, W. L. Fowler, Y. Li, J. S. Lee, L. Xing, R. H. Cheng, L. Wang, K. S. Lam, *Biomaterials* **2009**, *30*, 6006.
- [34] J. M. Chan, L. Zhang, K. P. Yuet, G. Liao, J.-W. Rhee, R. Langer, O. C. Farokhzad, *Biomaterials* **2009**, *30*, 1627.
- [35] T. Hamaguchi, K. Kato, H. Yasui, C. Morizane, M. Ikeda, H. Ueno, K. Muro, Y. Yamada, T. Okusaka, K. Shirao, Y. Shimada, H. Nakahama, Y. Matsumura, *Br. J. Cancer* **2007**, *97*, 170.
- [36] L. Huynh, C. Neale, R. Pomès, C. Allen, *Nanomedicine* **2012**, *8*, 20.
- [37] Z. Amoozgar, Y. Yeo, *Wiley Interdiscip. Rev. Nanomed. Nanobiotechnol.* **2012**, *4*, 219.
- [38] R. P. Garay, R. El-Gewely, J. K. Armstrong, G. Garratty, P. Richette, *Expert Opin. Drug Deliv.* **2012**, *9*, 1319.
- [39] Q. Yang, S. K. Lai, *Wiley Interdiscip. Rev. Nanomed. Nanobiotechnol.* **2015**, DOI: 10.1002/wnan.1339.
- [40] K. L. Eskow Jaunarajs, D. G. Standaert, T. X. Viegas, M. D. Bentley, Z. Fang, B. Dizman, K. Yoon, R. Weimer, P. Ravenscroft, T. H. Johnston, *Mov. Disord.* **2013**, *28*, 1675.
- [41] J. Tong, R. Luxenhofer, X. Yi, R. Jordan, A. V. Kabanov, *Mol. Pharm.* **2010**, *7*, 984.
- [42] J. Tong, X. Yi, R. Luxenhofer, W. A. Banks, R. Jordan, M. C. Zimmerman, A. V. Kabanov, *Mol. Pharm.* **2012**, *10*, 360.
- [43] S. Konieczny, C. P. Fik, N. J. Aversch, J. C. Tiller, *J. Biotechnol.* **2012**, *159*, 195.
- [44] C. P. Fik, C. Krumm, C. Muennig, T. I. Baur, U. Salz, T. Bock, J. C. Tiller, *Biomacromolecules* **2011**, *13*, 165.
- [45] Y. Chen, B. Pidhatika, T. von Erlach, R. Konradi, M. Textor, H. Hall, T. Lühmann, *Biointerphases* **2014**, *9*, 031003.
- [46] N. Zhang, T. Pompe, I. Amin, R. Luxenhofer, C. Werner, R. Jordan, *Macromol. Biosci.* **2012**, *12*, 926.
- [47] B. L. Farrugia, K. Kempe, U. S. Schubert, R. Hoogenboom, T. R. Dargaville, *Biomacromolecules* **2013**, *14*, 2724.
- [48] G. Hochleitner, J. F. Hümmer, R. Luxenhofer, J. Groll, *Polymer* **2014**, *55*, 5017.

- [49] T. von Erlach, S. Zwicker, B. Pidhatika, R. Konradi, M. Textor, H. Hall, T. Lühmann, *Biomaterials* **2011**, *32*, 5291.
- [50] Z. He, L. Miao, R. Jordan, D. Manickam, R. Luxenhofer, A. V. Kabanov, *Macromol. Biosci.* **2015**, DOI: 10.1002/mabi.201500021.
- [51] M. Barz, R. Luxenhofer, R. Zentel, M. J. Vicent, *Polym. Chem.* **2011**, *2*, 1900.
- [52] R. Luxenhofer, Y. Han, A. Schulz, J. Tong, Z. He, A. V. Kabanov, R. Jordan, *Macromolecular Rapid Communications* **2012**, *33*, 1724.
- [53] R. Luxenhofer, S. Huber, J. Hytry, J. Tong, A. V. Kabanov, R. Jordan, *J. Polym. Sci. A Polym. Chem.* **2013**, *51*, 732.
- [54] J.-S. Park, K. Kataoka, *Macromolecules* **2006**, *39*, 6622.
- [55] J.-S. Park, K. Kataoka, *Macromolecules* **2007**, *40*, 3599.
- [56] S. Huber, R. Jordan, *Colloid Polym. Sci.* **2008**, *286*, 395.
- [57] R. Hoogenboom, H. M. L. Thijs, M. J. H. C. Jochems, B. M. van Lankvelt, M. W. M. Fijten, U. S. Schubert, *Chem. Commun.* **2008**, 5758.
- [58] M. Foreman, J. Coffman, M. Murcia, S. Cesana, R. Jordan, G. Smith, C. Naumann, *Langmuir* **2003**, *19*, 326.
- [59] F. C. Gaertner, R. Luxenhofer, B. Blechert, R. Jordan, M. Essler, *J. Control. Release* **2007**, *119*, 291.
- [60] F. Rehfeldt, M. Tanaka, L. Pagnoni, R. Jordan, *Langmuir* **2002**, *18*, 4908.
- [61] R. Luxenhofer, M. Bezen, R. Jordan, *Macromol. Rapid Commun.* **2008**, *29*, 1509.
- [62] N. Zhang, S. Huber, A. Schulz, R. Luxenhofer, R. Jordan, *Macromolecules* **2009**, *42*, 2215.
- [63] N. Zhang, R. Luxenhofer, R. Jordan, *Macromol. Chem. Phys.* **2012**, *213*, 973.
- [64] N. Zhang, R. Luxenhofer, R. Jordan, *Macromol. Chem. Phys.* **2012**, *213*, 1963.
- [65] R. Luxenhofer, A. Schulz, C. Roques, S. Li, T. K. Bronich, E. V. Batrakova, R. Jordan, A. V. Kabanov, *Biomaterials* **2010**, *31*, 4972.
- [66] Y. Han, Z. He, A. Schulz, T. K. Bronich, R. Jordan, R. Luxenhofer, A. V. Kabanov, *Mol. Pharm.* **2012**, *9*, 2302.
- [67] A. Schulz, S. Jaksch, R. Schubel, E. Wegener, Z. Di, Y. Han, A. Meister, J. Kressler, A. V. Kabanov, R. Luxenhofer, C. M. Papadakis, R. Jordan, *ACS Nano* **2014**, *8*, 2686.
- [68] H. Witte, W. Seeliger, *Justus Liebigs Ann. Chem.* **1974**, *1974*, 996.
- [69] A. V. Kabanov, I. R. Nazarova, I. V. Astafieva, E. V. Batrakova, V. Y. Alakhov, A. A. Yaroslavov, V. A. Kabanov, *Macromolecules* **1995**, *28*, 2303.
- [70] R. Luxenhofer, G. Sahay, A. Schulz, D. Alakhova, T. K. Bronich, R. Jordan, A. V. Kabanov, *J. Control. Release* **2011**, *153*, 73.
- [71] Z. He, A. Schulz, X. Wan, J. Seitz, H. Bludau, D. Y. Alakhova, D. B. Darr, C. M. Perou, R. Jordan, I. Ojima, A. V. Kabanov, R. Luxenhofer, *J. Control. Release* **2015**, *208*, 67.
- [72] J. Luo, K. Xiao, Y. Li, J. S. Lee, L. Shi, Y.-H. Tan, L. Xing, R. Holland Cheng, G.-Y. Liu, K. S. Lam, *Bioconjug. Chem.* **2010**, *21*, 1216.
- [73] V. Alakhov, E. Moskaleva, E. V. Batrakova, A. V. Kabanov, *Bioconjug. Chem.* **1996**, *7*, 209.
- [74] E. V. Batrakova, A. V. Kabanov, *J. Control. Release* **2008**, *130*, 98.
- [75] S. Kobayashi, *Prog. Polym. Sci.* **1990**, *15*, 751.
- [76] T. X. Viegas, M. D. Bentley, J. M. Harris, Z. Fang, K. Yoon, B. Dizman, R. Weimer, A. Mero, G. Pasut, F. M. Veronese, *Bioconjug. Chem.* **2011**, *22*, 976.
- [77] R. W. Moadith, T. X. Viegas, D. G. Standaert, M. D. Bentley, Z. Fang, B. Dizman, K. Yoon, R. Weimer, J. M. Harris, P. Ravenscroft, T. H. Johnston, M. Hill, J. M. Brotchie, in 16th International Conference of Parkinson's Disease and Movement Disorders, Dublin, Ireland, **2012**.

SUPPORTING INFORMATION

Supporting information may be found in the online version of this paper.